**The 5th International Conference on Engineering Mechanics and Automation (ICEMA-5)**
**Hanoi, October 11÷12, 2019**

# Automated the QRS complex detection for monitoring the electrical activity of the heart

Manh Hoang Van[a], Viet Dang Anh[a], Quan Dang Hong[b] and Thang Pham Manh[a]

[a] *Lecturer, University of Engineering and Technology, Vietnam National University, Ha Noi*
[b] *Master student, University of Engineering and Technology, Vietnam National University, Ha Noi*

**Abstract**

In this work, we present a novel QRS complex detection approach in noisy exercise ECG signals based on a continuous wavelet transform (CWT) for a single-lead ECG signal. First, the adaptive filtering algorithm is employed to remove the additive artifacts from the signals. The ECG signals are then transformed by a CWT at a suitable scale. Finally, the QRS complex is detected in processed signals. The performance of the proposed algorithm is evaluated on the MIT-BIH Noise Stress Test Database. The recordings in this dataset are specially selected and characterized by baseline wander, muscle artifacts, and electrode motion artifacts as noise sources. Obtained results show that the proposed method reached the most satisfactory performance compared with several other QRS complex detection algorithms.

*Key Words: ECG, continuous wavelet transform, stress ECG test, RLS filter.*

## I. Introduction

The Electrocardiogram (ECG) is simply a recording of the electrical activity of the heart by electrodes placed on the surface of the body. Changes in the voltage measured by the electrodes are due to the action potentials of irritating heart cells that cause cell contractions. The resulting ECG heart cycle is represented by a series of waves whose morphology and occurrence time contain information utilized to diagnose cardiovascular diseases. However, the challenge when diagnosing heart diseases with ECG signals is that these signals vary considerably between different people. Besides, different patients might have various morphologies for the same condition. Also, two different diseases may have similarities in the properties of an ECG signal. These issues cause several difficulties for heart disease diagnosis [1][2]. To determine the abnormalities of the heartbeat, each beat of the ECG signal must be analyzed. The QRS complex is the essential waveform within the ECG signal since its shape provides much information about the current condition of the heart.

Within the last decade, many new approaches have been proposed to improve the accuracy of the QRS complex detector. The well-known Pan and Tompkins approach, which is based on the slope, amplitude, and width of the ECG signal [3]. After filtering the signal, smoothing the waveform, and emphasizing the QRS complex slope and width, the two threshold sets are applied to locate the true positive R peaks. An improved version of the Pan and Tompkins method is introduced in [4], where the process of calculating the threshold is optimized through analyzing three estimators (mean, median, and an iterative peak level). In [5], the authors proposed the real-time QRS complex detection approach consisting of four phases. First, the unwanted noises are removed from the ECG signals by using a band-pass filter. A five-point first-order differentiation, absolute and backward searching operation, was then utilized to improve the QRS complex. For an accurate determination of local maxima with different shapes, a K-nearest neighbor-based peak-finding and particle swarm optimization algorithm was implemented.

This paper aims to develop an algorithm to detect and localize QRS complexes in ECG signals during exercise by analyzing a wide range of other morphologies. The performance of the method is evaluated on reputable standard manually annotated MIT-BIH Noise Stress Test Database [6].

The remainder of this work is organized as follows: the proposed approach is introduced in Section II. Experimental results and performance are presented in Section III. The novelty and findings of this work are summarized in Section IV.

## II. Description of the proposed approach

The proposed wavelet-based algorithm for the detection of the QRS complex is presented in Figure 1. This method includes the signal preprocessing, the continuous wavelet transform, the thresholding and determination of candidate extremum pairs, and the identification of QRS complexes. The detail of each stage is described in the following sections.

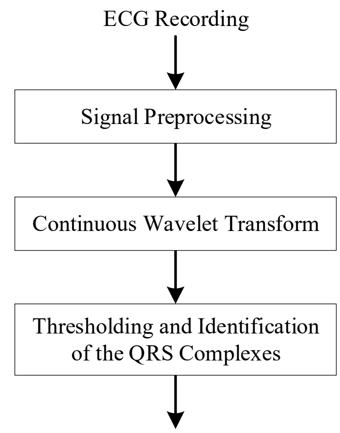


Figure 1. Block diagram of the proposed wavelet-based algorithm for the detection of the QRS complex.

### *1. Signal preprocessing*

Each ECG signal was first segmented by a sliding window of 4096 samples with an overlap of 150 samples between two adjacent windows, as shown in Figure 2. The design of the 150-sample overlap aims to avoid the incomplete QRS complexes located at the end of the 4096-sample segments, which could be misidentified as Not QRS complexes. Each section was then filtered by the adaptive filter algorithm to remove the Powerline Interference (PLI) and Baseline Wander (BW) noise from the ECG signals.

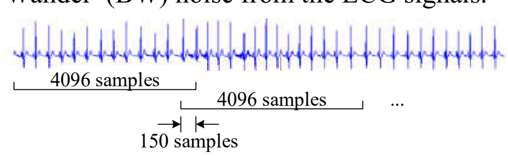


Figure 2. Illustration of segmentation of the ECG signal

### *2. Continuous wavelet transform*

In this work, the numerical realization of the CWT has been chosen because the execution speed of the algorithm will be faster. The wavelet transform (WT) describes a signal from a time-frequency perspective on different scales, with a different frequency band corresponding to each scale. While the dyadic form of discrete-time wavelet transform (DyDTWT) is limited to scales that are powers of two [9][10], the CWT can be calculated for any scale. Thus, a CWT-based approach is offered as an alternative tool to detect the QRS complexes in ECG signals. The use of the appropriate scales, the effects of interference, and signal fluctuations caused by breathing and patient movements during recording can be significantly reduced.

The CWT of the continuous signal $x(t)$ at the scale $a \in R^+$ and translational value $b \in R^+$ is expressed by the integral [10]

$$CWT(b, a) = \frac{1}{\sqrt{a}} \int_{-\infty}^{+\infty} x(t)\psi^*\left(\frac{t-b}{a}\right) dt \quad (1)$$

where $\psi(t)$ is a continuous function called the mother wavelet, and the asterisk denotes the operation of the complex conjugate.

The most commonly used types of mother wavelet for detecting the QRS complexes are the quadratic spline function [9][10] and the first derivative of the Gaussian function [11]. However, by experimenting with several other mother wavelets, especially from the biorthogonal family, we achieved the best results with $bior1.5$. In [9][10], the authors found the similarities across the other DyDTWT scales; our approach is based on finding and using an appropriate scale. The best results were achieved with the scale 15. The wavelet $bior1.5$ is an odd symmetry wavelet that transforms the extremes of the original signal into zero-level passages and transforms the inflection points into extremes. Thus, by transform, the signal is altered in a similar way to the derivative.

### *3. The thresholding and identification of the QRS complexes*

After the filtered signal is transformed by the CWT at the scale 15, the algorithm will search in the transformed signal of pairs of near opposite sign extremes, whose absolute values are greater than the threshold $\xi_{QRS}$. If such pairs of extremes are found, and if these extremes are spaced less than $120\,ms$, then the positions of these extremes correspond to the ascending and descending edges of several of the QRS complexes. The wave position is then determined by the zero-crossing position between the two adjacent extremes. In this way, one or more waves of the QRS complex can be detected. Because the detector indicates the location of the complex as a whole, it is necessary to select a single position representing the QRS complex. For this purpose, there is a refractory period $120\,ms$ before the next one can be detected since the QRS complexes cannot occur more closely than this physiologically. The positions preceded by another location in an interval shorter than the refractory period are removed from the detected positions. Therefore, the location of the QRS complex is the position of the first detected wave within the complex. The threshold level $\xi_{QRS}$ is given by the equation,

$$\xi_{QRS} = 1{,}6. \sqrt{\frac{1}{n}\sum_{i=1}^{n}(x_i - \bar{x})^2} \quad (2)$$

And thus, we can see that the threshold value corresponds to 1.6 times the standard deviation calculated from all the values of the transformed signal segment analyzed. The constant of 1.6 was determined as a suitable factor of the standard deviation based on the analysis of the complete ECG signal database (highest detection rate). Deriving a threshold level from a standard deviation is a more robust approach than a threshold derived from the maximum value or the difference between the maximum and the minimum that can easily be affected by the artifact or extrasystoles. The threshold is fixed, and its value is the same for the entire segment of the analyzed signal.

## III. Results and Discussion

### *1. The ECG database*

The proposed algorithm is evaluated using the MIT-BIH Noise Stress Test Database [6], which includes twelve half-hour ECG records and three half-hour records of noise typical in ambulatory ECG records. The ECG records were created by adding calibrated amounts of noise (baseline wander, electrode motion artifact, or muscle noise) to clean ECG recordings from the

MIT-BIH Arrhythmia Database [12]. To evaluate the performance of this work, only the files provided from the database (files 118 and 119) are used in the test. They are only affected by the artifact of EM type (electrode motion artifact noise).

The noise was added beginning after the first five minutes of each record, during two-minute segments, alternating with two-minute clean sections. The three noise signal records were assembled from the signal files by selecting parts that contained an electrode motion artifact. Since the original ECG recordings are clean, the correct beat annotations are known even when the noise makes the records visually unreadable. The reference annotations for these records are simply copies of those for the original clean ECG signals. The signal-to-noise ratios (SNRs) during the noisy segments of these records are listed in the flowing Table 1.

**Table 1.** The records in the MIT-BIH Noise Stress Test Database [13].

| Record | SNR (dB) | Record | SNR (dB) |
|---|---|---|---|
| 118e24 | 24 | 119e24 | 24 |
| 118e18 | 18 | 119e18 | 18 |
| 118e12 | 12 | 119e12 | 12 |
| 118e06 | 6 | 119e06 | 6 |
| 118e00 | 0 | 119e00 | 0 |
| 118e_6 | -6 | 119e_6 | -6 |

To compare the performance of our proposed algorithm with several other prominent QRS complex detectors specified in the literature, only the first channel of each ECG record is used.

*2. Performance evaluation and comparisons*

For the performance evaluation of the proposed method, the parameters such as sensitivity, positive prediction, and detection error rate are taken into account. The sensitivity ($Se$) is defined as the probability of detecting a QRS complex when a QRS exists; the positive prediction ($P^{+}$) represents the probability of detecting the QRS complex among the detected ECG peaks. They are calculated by using the following equations:

Sensitivity: $Se = \frac{TP}{TP+FN}$ (3)

Positive Prediction: $P^{+} = \frac{TP}{TP+FN}$ (4)

Detection Error Rate: $DER = \frac{FP+FN}{TP+FN}$ (5)

where, TP (the number of true positive detections) is the number of correct identified QRS complexes present in the signal under test; FN (stands for the amount of false-negative detections) is the number of QRS complexes present in the signal that the algorithm is not able to detect; FP (stands for the amount of false-positive misdetections) is the number of QRS complexes detected by the algorithm that are not actually in the signal.

To evaluate the accuracy of the detected QRS complex, a tolerance window of $150\ ms$, centered at the reference annotation, has been used. Different signal to noise ratio (SNR) levels for the same ECG record is analyzed; in particular, values ranging from $24\ dB$ to $0\ dB$ are tested. The performance of the proposed method related to different SNR levels of the same ECG signal is shown in Figures 3 and 4.

From the analytical figures, we can see that the sensitivity parameter is almost constant. Therefore, it is rather unaffected by artifact corrupting the ECG signal. The obtained results show that the algorithm is almost immune to noise up to SNR levels equal to 6 dB. Specifically, for SNR = 6 dB, the obtained $Se$ and $P^{+}$ values are 99.51% and 96.63%, respectively. For SNR levels lower than 6 dB, the parameters $Se$ and $P^{+}$ are dependent on the amount of noise. In particular, an assessment of the results achieved for SNR values equal to 0 dB, $Se$ and $P^{+}$ reach values of 95.97% and 88.61%, respectively.

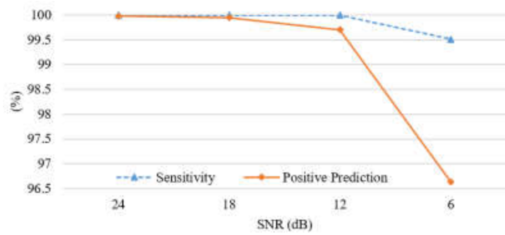


Figure 3. Algorithm behavior as a function of different SNR levels.

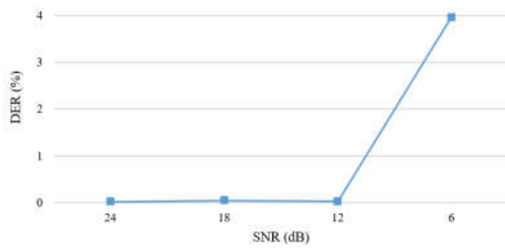


Figure 4. Detection error rate achieved as a function of different SNR levels.

To compare the performance of the proposed algorithm with several available works, the same test procedure indicated in the article [14] has been implemented. In [14], the authors have analyzed the algorithms in [15][16][17][11] for the assessment of their robustness against artifact using the MIT-BIH Noise Stress Test Database as a test bench. Table 2 shows a comparative study among the performance of the proposed method in this paper and the results of the algorithms, as reported in [13][14].

**Table 2.** The Se and $P^+$ values obtained using the MIT BIH Noise Stress Test Database, with an SNR = 6 dB and 0 dB.

| | SNR = 6 dB | | SNR = 0 dB | |
|---|---|---|---|---|
| **Method** | **Se** | **$P^+$** | **Se** | **$P^+$** |
| This work | 99.51 | 96.63 | 95.97 | 88.61 |
| Pangerc U. et al. | 99.91 | 95.91 | 83.97 | 68.92 |
| De Cooman T. et al. | 99.47 | 73.30 | 96.51 | 59.36 |
| Vollmer M. | 98.50 | 96.73 | 77.10 | 74.91 |
| Matteo D'Aloia et al. | 98.13 | 96.91 | 78.98 | 75.25 |
| Antink C.H. et al. | 84.89 | 76.40 | 72.20 | 66.37 |

The data table indicates that our proposed algorithm has good results compared to other algorithms shown in the literature. More specifically, it achieves the most effective $P^+$ value compared to all the analyzed methods for SNR value equal to 0 dB.

## IV. Conclusion

This paper introduces an innovative approach to the detection of QRS complexes in noisy exercise ECG signals. The method is based on the numerical implementation of the continuous wavelet transform, an appropriate choice of mother wavelet and scale used, thresholding with a fixed threshold.

The MIT-BIH Noise Stress Database was employed to evaluate the noise robustness of the proposed algorithm. Experimental results indicate that the algorithm can still obtain good results when the SNR level is up to 6 dB. For SNR levels lower than 6 dB, the achieved results get worse, since an increase of the FP and FN is observed.

## V. Acknowledgment

This work is supported by the research project N0. 01C02/01-2016-2 granted by the Department of Science and Technology Hanoi.

## VI. References

[1] J. Mateo, A. M. Torres, A. Aparicio, and J. L. Santos, "An efficient method for ECG beat classification and correction of ectopic beats," *Comput. Electr. Eng.*, vol. 53, pp. 219–229, 2016.

[2] S. Shadmand and B. Mashoufi, "A new personalized ECG signal classification algorithm using Block-based Neural Network and Particle Swarm Optimization," *Biomed. Signal Process. Control*, vol. 25, pp. 12–23, 2016.

[3] J. Pan and W. J. Tompkins, "A Real-time {QRS} Detection Algorithm," *IEEE Trans. Biomed. Eng.*, vol. 32, no. 3, pp. 230–236, 1985.

[4] P. S. Hamilton and W. J. Tompkins, "Quantitative Investigation of QRS Detection Rules Using the MIT/BIH

Arrhythmia Database," *IEEE Trans. Biomed. Eng.*, vol. BME-33, no. 12, pp. 1157–1165, Dec. 1986.

[5] R. He *et al.*, "A novel method for the detection of R-peaks in ECG based on K-Nearest Neighbors and Particle Swarm Optimization," *EURASIP J. Adv. Signal Process.*, vol. 2017, no. 1, 2017.

[6] G. B. Moody, W. K. Muldrow, and R. G. Mark, "Noise Stress Test for Arrhythmia Detectors.," *Computers in Cardiology*. pp. 381–384, 1984.

[7] G. D. Clifford, F. Azuaje, and P. E. McSharry, "Advanced Methods and Tools for ECG Data Analysis," *Adv. Methods Tools ECG Data Anal.*, pp. 1–400, 2006.

[8] P. L. and T. Hill, "Statistics : Methods and Applications By Pawel Lewicki and Thomas Hill," *Statistics (Ber).*, vol. 1st, pp. 1–719, 2006.

[9] C. Li, C. Zheng, and C. Tai, "Detection of ECG characteristic points using wavelet transforms," *IEEE Trans Biomed Eng*, vol. 42, no. Bmei, pp. 21–28, 1995.

[10] J. P. Martínez, R. Almeida, S. Olmos, A. P. Rocha, and P. Laguna, "A Wavelet-Based ECG Delineator Evaluation on Standard Databases," *IEEE Trans. Biomed. Eng.*, vol. 51, no. 4, pp. 570–581, 2004.

[11] M. Vollmer, "Robust detection of heart beats using dynamic thresholds and moving windows," *Comput. Cardiol. (2010).*, vol. 41, no. January, pp. 569–572, 2014.

[12] G. B. Moody and R. G. Mark, "The impact of the MIT-BIH arrhythmia database," *IEEE Eng. Med. Biol. Mag.*, vol. 20, no. 3, pp. 45–50, 2001.

[13] M. D'Aloia, A. Longo, and M. Rizzi, "Noisy ECG signal analysis for automatic peak detection," *Inf.*, vol. 10, no. 2, pp. 1–12, 2019.

[14] M. Vollmer, "Noise resistance of several top-scored heart beat detectors," *Comput. Cardiol. (2010).*, vol. 44, no. April, pp. 1–4, 2017.

[15] C. H. Antink, C. Brüser, and S. Leonhardt, "Detection of heart beats in multimodal data: A robust beat-to-beat interval estimation approach," *Physiol. Meas.*, vol. 36, no. 8, pp. 1679–1690, 2015.

[16] T. De Cooman, G. Goovaerts, C. Varon, D. Widjaja, T. Willemen, and S. Van Huffel, "Heart beat detection in multimodal data using automatic relevant signal detection," *Physiol. Meas.*, vol. 36, no. 8, pp. 1691–1704, 2015.

[17] U. Pangerc and F. Jager, "Robust detection of heart beats in multimodal records using slope- and peak-sensitive band-pass filters," *Physiol. Meas.*, vol. 36, no. 8, pp. 1645–1664, 2015.